

JAN SZANTYR, Assist.Prof., D.Sc., N.A.
 TADEUSZ BUGALSKI, D.Sc., N.A.
 Polish Academy of Sciences
 Institute of Fluid Flow Machinery
 Gdańsk

Numerical analysis of flow inside a waterjet

SUMMARY

The paper presents a numerical method for analysis of flow inside waterjets. The method is based on modelling the waterjet intake, channel and outlet by a discrete distribution of sources and modelling the impeller, guide vanes and other lifting elements by a lifting surface comprising discrete distribution of vortices and sources/sinks. The method is intended to predict flow streamlines and velocity distribution, pressure distribution, hydrodynamic forces and presence of cavitation on elements of a waterjet of a given geometry and prescribed operational parameters. Numerical results are compared with the data acquired during a specially arranged series of experiments with a waterjet model installed on top of a cavitation tunnel.

The paper presented at International Conference on Problems of Marine Propulsion HYDRONAV '95, Gdańsk, November 1995

INTRODUCTION

Marine propellers are usually designed individually for any particular ship and the process of their design is in fact quite an involved interaction between shipowner, shipyard, model basin and propeller designer. This process leaves an ample room for evolution, modification, tests and „second thoughts” on the part of all involved. On the contrary, waterjets are usually bought „off the shelf” from a specialist manufacturer which employs a rather limited amount of information about the vessel for selecting an appropriate model of the propulsor from his production range. This approach is justified by a well-known flexibility of the hydrodynamic characteristics of waterjets. However, as the unit power of waterjets is rapidly growing, a number of full-scale problems with these propulsors, including cavitation erosion, is increasing. Consequently, there is a need for development of an analytical method for the calculation of flow inside a waterjet of arbitrary geometry, which would enable to eliminate some of these problems at a design stage.

Research project presented in this paper was devoted to development of such a method which could be used in the form of a computer program for analysis of flow, calculation of time-dependent pressure distribution, resulting hydrodynamic forces and cavitation inception for a waterjet of a given geometry and operating characteristics. Apart from purely theoretical development the project included an experimental part in which a model of waterjet with three optional intakes was to be constructed and tested on top of the cavitation tunnel.

THEORETICAL MODEL USED IN THE NUMERICAL METHOD

The well-known Hess & Smith method, described in [3], is used for modelling the potential flow inside the waterjet. The internal surface of the waterjet inlet, channel and outlet is modelled by a number of flat quadrangle panels, shown in Fig.1. In standard configuration 720 panels are used with 24 of them located in each of 30 annular sections. Normally it is assumed that the circumference of each annular section is divided into 24 equal panels. The distribution of panels depends in each case on the detail geometry of the waterjet and is based on two contradictory principles:

- panel distribution should be more dense in the region of marked geometry variation
- size of adjacent panels should not differ too much, e.g. $\pm 25\%$ of the area

The Hess&Smith method is based on determination of the distribution of sources which satisfies the classical kinematic boundary condition of no flow through the modelled surface. It is a first order method, i.e. it is assumed that distribution of sources is uniform on each panel. This leads to the system of Fredholm equations of the second kind for the unknown intensity of sources:

$$\sum_{j=1}^N A_{ij} \sigma_j = -n_{xi} V_i \quad i = 1 \dots N \quad (1)$$

The coefficients A_{ij} of the system of equations (1) are determined through calculation of the velocity induced by the source located on j-th panel in the control point of i-th panel. The right hand side of (1) expresses the condition of impermeability of the channel walls for the flow fulfilling the continuity equation. The velocity induced by lifting elements of the waterjet may be also included in the right hand side of (1) at appropriate stages of analysis of flow through the complete propulsor.

When the above system of linear equations is solved by the direct Gauss elimination method, the velocity distribution on channel walls and at the selected points inside the channel may be determined. In particular, the velocity induced at the control points of the lifting elements of the waterjet may be calculated.

The parameters of the potential flow inside the waterjet channel are further used for determination of the turbulent boundary layer on the inside surface of the channel. This is presently being done by means of the very simple „short cut” methods adapted from [1]. They enable to estimate the velocity profile inside the waterjet and assess the blockage effect due to the presence of the boundary layer inside the channel.

It is assumed that a waterjet propulsor may have a number of rotating and/or stationary lifting elements inside it, such as shaft supports, impeller and guide vanes. It is further assumed that the shaft support may consist of up to four foils of different geometry while both impeller and guide vane system may consist of up to twelve identical, equally spaced foils (blades). All lifting elements are modelled by lifting surface theory, essentially following the approach described in [2] and [4].

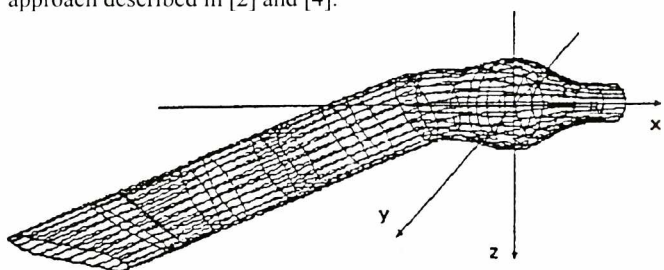


Fig. 1. Discrete model of the waterjet channel

An example of application of the lifting surface to modelling the impeller blade is shown in Fig.2. The lifting surface is based on simulating the hydrodynamic loading on the foils with the appropriate distribution of vorticity and simulating the foil thickness with the appropriate distribution of sources and sinks. Both these types of singularities are distributed on mean surfaces of respective foils. Following the classical linearized approach it is assumed that the effects of foil loading and thickness may be separated from each other.

The kinematic boundary condition is the basis for formulation of the lifting surface equation. This condition requires that the resultant relative velocity of flow at the lifting surface should be tangent to this surface. This leads to the following integral equation:

$$(2)$$

$$\frac{1}{4\pi} \left[\iint_{S_p} \vec{n} \cdot \vec{\gamma}_p \nabla \left(-\frac{1}{r_p} \right) dS + \iint_{S_s} \vec{n} \cdot \vec{\gamma}_s \nabla \left(-\frac{1}{r_s} \right) dS + \iint_{S_p} q_p \frac{\partial}{\partial n} \left(-\frac{1}{r_p} \right) dS \right] + (\vec{V} + \vec{\omega}R) \cdot \vec{i} = 0$$

In numerical evaluation of equation (1) the continuous distribution of vorticity and sources over the lifting surfaces is replaced by a discrete distribution of concentrated vortex and source elements, as shown in Fig.2. The boundary condition is evaluated in a number of control points distributed over the surface between the vortex elements. Typically, 72 control points and 80 bound vortex elements/source elements are on each foil. As each of the control points generates one equation it is necessary, in order to obtain a closed system of linear equations for unknown intensity of bound vortex elements, to employ Kutta condition at the trailing edge of each foil.

Each lifting surface has to be supplemented with a system of free vortices shed from its trailing edge. This system looks differently for each internal lifting element of a waterjet. For shaft support, which is generally located close to the inlet, this system is aligned with the flow inside the waterjet and its vortex lines extend up to the leading edge of the impeller. As the impeller is usually followed by the system of guide vanes, the free vortex system of impeller is very short (cf. Fig.2). The system of free vortices behind guide vanes is aligned with the flow and it extends downstream for a distance corresponding to one revolution of the rotor, which in most cases means leaving the outlet nozzle.

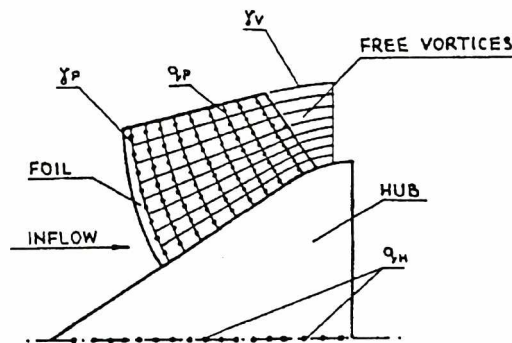


Fig. 2. Discrete model of the impeller

The hub linking impeller with the guide vanes is usually quite substantial and its influence on the flow can not be neglected. In the present method the hub is modelled by a distribution of sources and sinks along its axis.

Solution of the system of linear equations resulting from the boundary condition for any one of the lifting elements of the waterjet leads to determination of intensity of bound vortex elements on the lifting surfaces. Normally such a solution takes into account velocities induced by all other parts of the waterjet, which is explained in a greater detail below. Once the solution is obtained, the resultant tangential velocity distribution on both sides of the lifting surface may be calculated and the pressure distribution follows the Bernoulli equation. This pressure distribution is corrected for the effect of viscosity by means of empirical coefficients and for effect of leading edge singularity by means of the Lighthill formula [5]. The corrected pressure distribution is employed to assess cavitation inception. This is being done presently by means of a rather crude assumption that cavitation starts when static pressure drops below critical pressure, but it is planned to refine this section of the algorithm in the near future. The calculated pressure distribution is also employed to evaluate forces on all lifting elements inside the waterjet. This is done by means of the following formulae defined in the system of coordinates shown in Fig. 1:

$$F_x = \frac{1}{2} \rho V_\infty^2 \iint_{S_p} (\Delta C_p n_x + C_D t_x) dS \quad (3)$$

$$M_x = \frac{1}{2} \rho V_\infty^2 \iint_{S_p} [(\Delta C_p n_z + C_D t_z) y - (\Delta C_p n_y + C_D t_y) z] dS \quad (4)$$

The other components of the hydrodynamic loading may be calculated by means of analogical formulae. The sectional drag coefficient is derived from empirical data.

When the vorticity distribution on any one of the lifting elements has been determined, the velocity induced by this element on other elements may be easily calculated. This velocity is included in the boundary condition on these elements at an appropriate stage of the analysis of flow through the complete waterjet.

GENERAL STRUCTURE OF THE COMPUTER PROGRAM

Complicated mutual interaction between all elements of the waterjet such as channel, impeller, guide vanes etc. requires appropriate structure of the calculation process. The block diagram of the process, which is simultaneously the diagram of the corresponding computer program, is shown in Fig.3. The calculation starts with introduction and transformation of the given waterjet geometry. This is done separately for each of the elements (the PK1, PW1, PR1, PS1 subroutines) and all internal elements may be optionally excluded from the analysis. Transformation of the geometry means in fact generation of complete discrete vortex/source models of respective elements.

In the next group of calculations the induction factors matrices are evaluated for all elements of the waterjet. This is done by means of the Biot-Savart formula in the separate subroutines PW2, PR2, PS2 for shaft support, impeller and guide vanes system respectively,

and by means of point source potential in PK2 for the channel. The induction matrices are arrays of coefficients linking intensity of discrete vortices (or sources) with velocities induced by them in control points. Consequently, these matrices contain the essence of geometry of the complete waterjet propulsor. There are separate matrices for induction from any element on itself and on all other elements and separate matrices for every required component of the induced velocity. Simultaneously velocities induced by source/sink systems on all lifting elements are calculated.

Then the process of calculating the flow through the waterjet begins. The first round of this process starts with calculation of the flow through the waterjet channel without any interaction from the lifting elements (the FK1 subroutine). As a result the induction from the channel on all lifting elements of the waterjet is determined. Then the kinematic boundary condition on the shaft support (if present - the FW1 subroutine) is solved and induction from it on the channel and remaining lifting elements is determined together with pressure distribution and resulting hydrodynamic forces on the shaft support foils. Next the kinematic boundary condition on the impeller in the circumferentially averaged flow is solved in the FR1 subroutine, taking into account velocity induced by the channel and shaft support (if present). This leads to determination of pressure distribution and resulting hydrodynamic forces on the impeller blades, together with induction from it on the channel, shaft support and guide vane system.

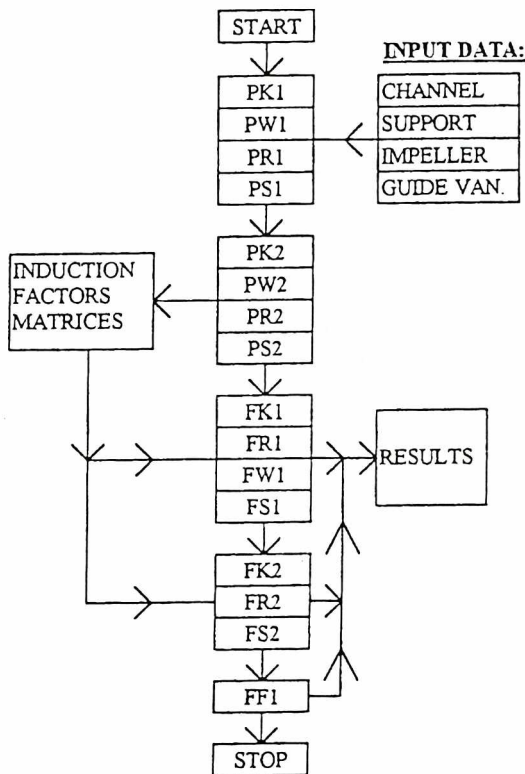


Fig. 3. Block diagram of the numerical method

This round of calculation is completed with solution of the kinematic boundary condition on the guide vane system in the FS1 subroutine, taking into account induction from the channel, shaft support and impeller. Pressure distribution, hydrodynamic forces and induction from guide vanes on all other elements of the waterjet result from this calculation.

In the next round the flow through the channel is solved again (the FK2 subroutine), this time taking into account velocities induced by all lifting elements located inside it. This leads to more accurate determination of the induction from the channel on impeller and guide vanes. Now the analysis of the flow at impeller in a series of specified angular positions, including interaction with the guide vanes, is performed using the FR2 and FS2 subroutines. Finally, the harmonic analysis of fluctuating hydrodynamic forces on the impeller and guide vanes is performed by the FFI subroutine.

The computer program based on the above described sequence of calculations has been written in Fortran for execution on PC computers. A complete analysis of the waterjet on a 66MHz machine

requires about 25 minutes. The program is still in the process of validation by means of comparison of its results with available experimental data.

EXPERIMENTS WITH A WATERJET MODEL

As the experimental data were necessary for validation of the theoretical method, a special model of a waterjet propulsor has been constructed and installed on top of the Kempf&Remmers K11 cavitation tunnel in the laboratory of IFFM.

The prime target of the experiment was to measure velocity distribution inside the waterjet at several selected positions and to measure thrust, torque and rotational speed of the impeller. The main body of the waterjet was built of glass-reinforced plastic and enclosed by a steel casing. Inside the waterjet the bronze five-bladed diagonal impeller and six-bladed guide vane system were installed (see Fig.4).

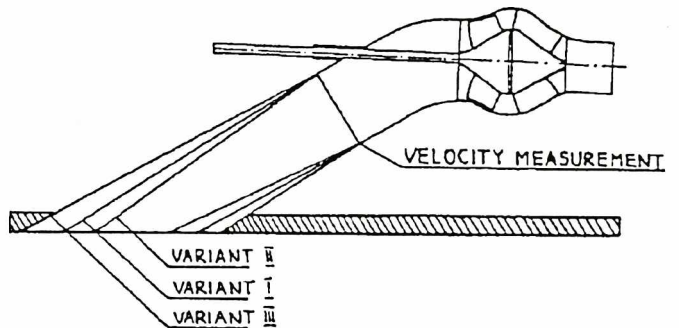


Fig. 4. Scheme of the waterjet model

The outer diameter of the impeller was 120 mm and the maximum hub diameter was 80 mm. Three exchangeable inlet ducts with different cross-sections at entrance have been designed: circular cross-section (Variant I), quasi-elliptical cross-section with long axis perpendicular to inflow (Variant II), and quasi-elliptical cross-section with long axis in the direction of inflow (Variant III). Both Variant II and III had the ratio between long and short axis equal to 2,0 and the area of inlet cross-section was the same in all three variants. The velocity inside the waterjet was measured by three-hole probes which were inserted through special sockets installed in the waterjet channel and equipped with devices for controlling their positioning. Pressure was converted into electrical signals by means of a strain gauge sensor.

The experimental program included the following measurements for each variant of the inlet nozzle:

- measurement of three components of velocity at 20, 40 points inside the waterjet (depending on the variant)
- measurement of thrust and torque of the impeller

The above stated measurements have been performed for three operating conditions described by pairs of numbers giving tunnel velocity and impeller rotation:

4,7 m/s; 2000 rpm
 approx. 5,5 m/s; 2500 rpm
 approx. 5,85 m/s; 3000 rpm

COMPARISON OF NUMERICAL AND EXPERIMENTAL RESULTS

The comparison of calculated and experimentally measured velocity of flow in the selected points inside the waterjet is presented in Figs. 5, 6 and 7 for the inlet variants I, II and III respectively. All data refer to the cross-section indicated in Fig. 4. The results presented in Figs. 5, 6 and 7 correspond to impeller speed 2500 rpm and velocity in the cavitation tunnel of 5,5 m/s. The measured velocity profiles are generally quite well reproduced in calculation.

CONCLUSIONS

The following conclusions may be drawn in order to summarize the above presented research project:

- the initial experimental validation has confirmed the basic assumptions of the analytical method
- the presented analytical method requires further development, in particular concerning viscous flow analysis and boundary layer modelling
- further experimental verification is necessary, especially in relation to cavitation and unsteady hydrodynamic forces
- the method represents a perspective useful tool for designers of waterjet-propelled vessels

Acknowledgements

The research project described in this paper has been financed by the Polish Scientific Research Committee grant No. 0404/S6/93/05, which is gratefully acknowledged. The authors are indebted to Mr. J. Koronowicz and Dr. L. Wilczynski of IFFM for preparation and execution of the experiments.

NOMENCLATURE

- A_{ij} - coefficients of the system of linear equations
- C_D - sectional drag coefficient
- ΔC_p - difference of pressure acting on the lifting surface element dS
- F_x - foil thrust
- M_x - foil torque
- n_x, n_y, n_z - components of the local normal unit length vector
- \vec{n} - unit length vector normal to the lifting surface
- q_p - source/sink distribution on the lifting surface
- R - radius on which control point is located
- r_p - distance between control point and vortex/source element
- S_p - lifting surface area
- S_v - free vortex surface area
- t_x, t_y, t_z - components of the local tangential unit length vector
- V - axial inflow velocity at impeller/guide vanes
- V_j - inflow velocity at waterjet channel
- γ_p - vorticity distribution on the lifting surface
- γ_v - vorticity distribution on the free vortex surface
- $\bar{\omega}$ - angular velocity of impeller rotation
- σ_{ij} - intensity of sources at waterjet channel

BIBLIOGRAPHY

1. Cebeci T., Smith A.M.O.: "Analysis of Turbulent Boundary Layers". Academic Press Inc., New York, 1974
2. Glover E.J., Szantyr J.A.: "The Analysis of Unsteady Propeller Cavitation and Hull Surface Pressures for Ducted Propellers". Trans. RINA, vol.132, 1990
3. Hess J.L., Smith A.M.O.: "Calculation of Potential Flow About Arbitrary Bodies"; in: "Progress in Aeronautical Sciences", Vol.8. Pergamon Press, Oxford, 1966
4. Szantyr J.A.: "A Method for Analysis of Cavitating Marine Propellers in Non-uniform Flow". International Shipbuilding Progress, Vol. 41, 1994, No. 427
5. Thwaites B.: "Incompressible Aerodynamics". At the Clarendon Press, Oxford, 1960

Appraised by Henryk Jarzyna, Prof., D.Sc., N.A.

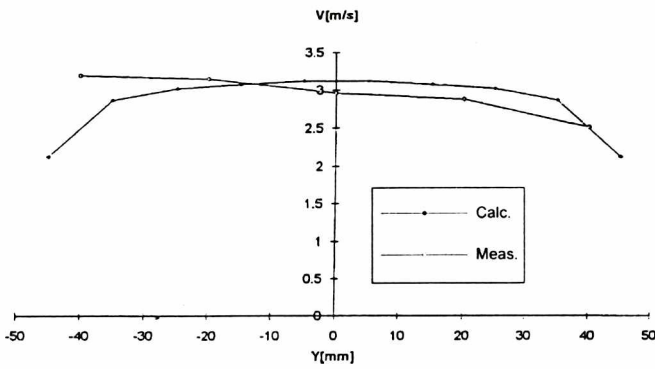


Fig. 5. Comparison of Calculated and Measured Velocities Inside Channel for Variant I

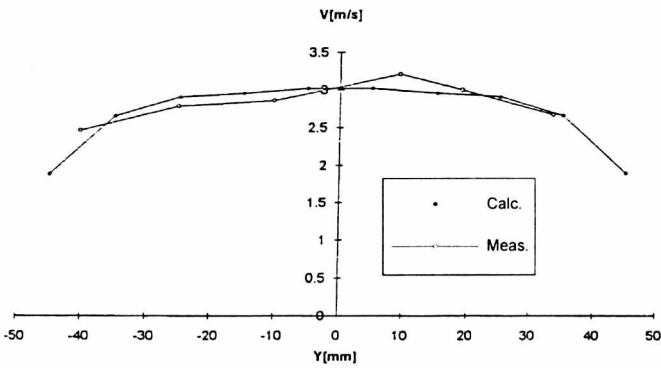


Fig. 6. Comparison of Calculated and Measured Velocities Inside Channel for Variant II

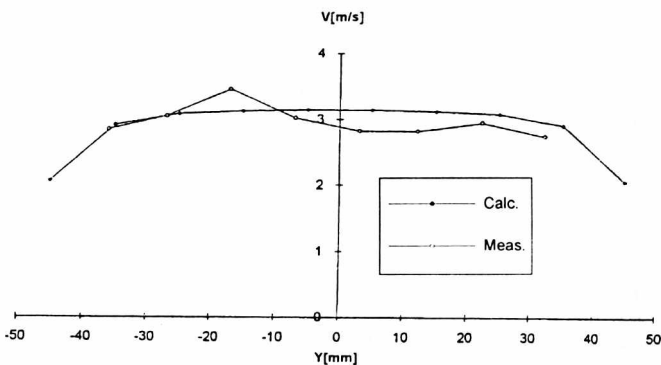


Fig. 7. Comparison of Calculated and Measured Velocities Inside Channel for Variant III

The results of calculation and measurement of the impeller thrust and torque are collected in Tab. 1 and 2 respectively. Although in individual points the discrepancy between calculation and experiment reaches 15%, the analytical method seems to reproduce the distinction between inlet variants reasonably well. The agreement is usually better for higher impeller rpms and/or in-tunnel velocities. The discrepancies visible in Tab. 1 and 2 may result from rather simple modelling of the boundary layer inside the waterjet and simple empirical correction for viscosity effect on the impeller pressure distribution.

Tab. 1. Comparison of the Measured and Calculated Impeller Thrust [N]

Impeller [rpm]	Velocity in tunnel [m/s]	Variant I		Variant II		Variant III	
		Meas.	Calc.	Meas.	Calc.	Meas.	Calc.
2000	4.7	93.6	90.2	105.6	91.0	104.8	90.6
2500	5.5	164.8	154.3	162.0	153.2	172.0	158.4
3000	5.85	230.0	237.2	238.0	241.2	250.0	245.0

Tab. 2. Comparison of the Measured and Calculated Impeller Torque [Nm]

Impeller [rpm]	Velocity in tunnel [m/s]	Variant I		Variant II		Variant III	
		Meas.	Calc.	Meas.	Calc.	Meas.	Calc.
2000	4.7	2.64	2.14	2.28	2.10	2.76	2.16
2500	5.5	4.24	4.02	3.72	3.99	4.60	4.08
3000	5.85	6.10	6.31	5.68	6.13	6.50	6.58